Flexible Extended Nested Array with Multiple Subarrays Achieving Improved Degrees of Freedom

Steven Wandale[1] and Koichi Ichige[2]
Department of Electrical and Computer Engineering, Yokohama National University
79-5 Tokiwadai, Hodogaya-ku, Yokohama 240-8501, Japan.
[1]wandale-steven-vf@ynu.jp,[2]koichi@ynu.ac.jp

***Abstract*—This paper proposes a new extended nested array geometry with enhanced degrees of freedom (DOF) and a hole-free difference co-array. The proposed flexible extended nested with multiple subarrays (f−ENAMS) configuration is constructed by splitting the dense subarray of the nested array (NA) into four subarrays and relocating them on either side of the NA configuration to maximize the DOF. Several conditions are provided for a specific design to guarantee the continuity of the difference co-array (DCA). Compared to other sparse arrays, f−ENAMS offers improved DOF, which leads to high-resolution DOA estimation. Simulation examples are presented to demonstrate the superiority of the proposed f−ENAMS array configuration.**

***Index Terms*—Extended nested array, direction-of-arrival estimation, degrees-of-freedom, mutual coupling.**

I. Introduction

Recently, non-uniform linear arrays (also known as sparse arrays) have become more attractive than conventional uniform linear arrays (ULAs) for several reasons [1]–[4]. To begin with, in the view of the difference coarray (DCA) concept, sparse arrays can achieve enhanced DOFs from $O(N)$ to $O(N^2)$, and are, hence, able to resolve more uncorrelated sources than the number of sensors [5]–[6]. Also, the larger intersensor spacing between the sparse array sensors reduces the mutual coupling (MC) effect between sensors compared to their conventional ULA counterparts [6]. There are different approaches to realizing such arrays, and the most prevalent ones include (a) the use of machine learning and evolutionary search-based algorithms to synthesize sparse arrays dynamically for joint properties such as hole-free co-arrays, low peak side lobes, and optimum far-field performance [7]–[9], and (b) the design of static sparse arrays with closed-form expressions for joint requirements like hole-free co-arrays and fewer mutual coupling effects [5]–[6], [10]–[20]. In this paper, however, we focus on the latter.

Sparse arrays that are well-known include minimum redundancy arrays (MRAs) [3], minimum hole arrays (MHAs) [4], coprime arrays (CAs) [5], and nested linear arrays (NAs) [6]. Despite their popularity, the MRA and MHA do not have closed-form expressions for sensor locations [4]–[6]. The CAs have holes in their DCAs, and therefore, the realized DOF is less than that of MRA and NA [6]. Also, NA has a severe mutual coupling effect owing to the existence of a dense ULA [10]. As a result, numerous variants of the NA and CA arrays have been proposed to either enhance the DOF or reduce the mutual coupling effect further [11]–[20]. For instance, variants such as the super nested array (SNA) [10], and generalized nested array (GNA) [11] were proposed to reduce the mutual coupling effect, whereas generalized coprime array (GCA) [12], thinned coprime array (TCA) [13], augmented nested array (ANA) [14], enhanced nested array (ENA) [15], improved nested array (INA) [16], Iizuka NA [17] and one or two-side extended nested array (OS/TS-ENA) [18] were proposed to improve the DOF.

Interestingly, some, like the sparse array with the maximum interelement spacing constraint (MISC) [19] achieve both improved DOF and less MC effect. In [20], we proposed extended nested array geometry with multiple subarrays (ENAMS). Although ENAMS has all the good properties of NA, and enhanced DOF, the realized DOF is still limited compared to MISC and OS/TS-ENA arrays. This indicates that there is still substantial potential for improvements regarding either enhancement of DOF or reduction of MC effect of prototype sparse arrays such as a nested array, coprime array, and ENAMS array.

This paper proposes a flexible extended nested with multiple subarrays (f−ENAMS) configuration with improved DOF. The proposed f−ENAMS is constructed by splitting the dense subarray of the NA into four subarrays and relocating them on either side of the NA configuration to maximize the DOF. This work extends the work in [20], where an extended nested array with multiple subarrays (ENAMS) is derived. More importantly, f−ENAMS has a closed-form expression for sensor positions and corresponding achievable DOF. Simulation examples are presented to validate the merits of the proposed extended nested arrays in terms of maximum DOF and DOA estimation performance.

Section II describes the co-array signal model. Section III describes the f−ENAMS array design, and Section IV explores DOA estimation examples with f−ENAMS. Section V concludes this work.

Notations: Operator vec$(\cdot)$ and diag$(\cdot)$ denote vectorization operation and diagonal matrix, respectively. $\otimes$ is the Kronecker product and $E[\,\cdot\,]$ is a statistical expectation operator. The $\xi(\mathbb{A}) = \{a_i - b_j | a_i, b_j \in \mathbb{A}\}$ and $\xi(\mathbb{A}, \mathbb{B}) = \{a_i - b_j | a_i \in \mathbb{A}, b_j \in \mathbb{B}\}$ denote self-difference set and cross-difference set, respectively. $\langle r_1, r_2 \rangle$ presents an integer set

This work was partly supported by the Japan Society for the Promotion of Science (JSPS) Grant-in-Aid for Scientific Research #20K04500. The authors are sincerely thankful for their support.

$\{r \in \mathbb{S} | r_1 \leq r \leq r_2\}$ and $\mathbb{S} = \{0, \pm 1, \pm 2, \ldots\}$.

II. Difference Co–Array Signal Model

Consider a sparse linear array (SLA) with $N-$sensors, whose sensor positions are $n_i d$ where n_i belongs to $\mathbb{S} = \{n_i\}_{i=1}^{N}$ and $d = \lambda/2$ is the unit intersensor spacing, with λ being the wavelength of the carrier frequency [1]. Assume K uncorrelated narrowband far-field sources from directions $\theta_k, k = 1, 2, ..., K$ are impinging on a SLA [2]–[5]. Then, the received signal vector at time t can be expressed as

$$\boldsymbol{x}(t) = \boldsymbol{B}\boldsymbol{s}(t) + \boldsymbol{n}(t), \tag{1}$$

such that $\boldsymbol{s}(t) = [s_1(t), s_2(t), \ldots, s_K(t)]^T$ is the signal vector and $\boldsymbol{n}(t)$ denotes the zero mean white Gaussian noise vector with variance $\sigma_n^2 \boldsymbol{I}_N$, where σ_n^2 is the noise power. Moreover, $\boldsymbol{B} = [\boldsymbol{b}(\theta_1), \boldsymbol{b}(\theta_2), \ldots, \boldsymbol{b}(\theta_K)]$ is the array manifold whose k-th source steering vector $b(\theta_k)$ can be expressed as

$$\boldsymbol{b}(\theta_k) = [e^{j\pi d_1 \sin(\theta_k)}, e^{j\pi d_2 \sin(\theta_k)}, \ldots, e^{j\pi d_N \sin(\theta_k)}]^T. \tag{2}$$

The covariance of $\boldsymbol{x}(t)$ can be defined as

$$\boldsymbol{R}_{xx} = E\big[\boldsymbol{x}(t)\boldsymbol{x}^H(t)\big] = \boldsymbol{B}\boldsymbol{R}_s\boldsymbol{B}^H + \sigma_n^2 \boldsymbol{I}_N, \tag{3}$$

where $\boldsymbol{R}_s = E\big[\boldsymbol{s}(t)\boldsymbol{s}^H(t)\big] \approx \text{diag}([\rho_1^2, \rho_2^2, \ldots, \rho_K^2])$ is the signal covariance matrix and ρ_k^2 denotes the signal power. In practice, the sampled snapshots are limited as such (3) can be approximated as

$$\hat{\boldsymbol{R}}_{xx} = \frac{1}{T}\sum_{t=1}^{T} \boldsymbol{x}(t)\boldsymbol{x}^H(t), \tag{4}$$

where T is the number of snapshots. According to [21]–[22], vectorizing (3) yields

$$\boldsymbol{y} = \text{vec}(\hat{\boldsymbol{R}}_x) = (\boldsymbol{B}^* \odot \boldsymbol{B})\boldsymbol{p}_c + \sigma_n^2 \boldsymbol{1}_N, \tag{5}$$

where $\boldsymbol{1}_N = \text{vec}(\boldsymbol{I}_N)$, and $(\boldsymbol{B}^* \odot \boldsymbol{B})$ denotes the extended array manifold of difference co-array $\mathbb{D}$. The DCA is defined as the difference in sensor positions of a sparse array $\mathbb{S}$ [5]. Namely,

$$\mathbb{D} = \{n_1 - n_2 | n_1, n_2 \in \mathbb{S}\}. \tag{6}$$

The repeated and discrete lags in $\boldsymbol{y}$ are sorted and removed. Then, a spatial-smoothing MUSIC (SS-MUSIC) [21] can be used to estimate DOAs.

Definition 1. *(Uniform DOF): Given a sparse array $\mathbb{S}$ and corresponding DCA $\mathbb{D}$, the consecutive co-array $\mathbb{U}$ can be given as*

$$\mathbb{U} = \langle -R_u, R_u \rangle \subseteq \mathbb{D}, \tag{7}$$

where $-R_u$ and R_u restrict the range of the consecutive co-array $\mathbb{U}$. Thus, the cardinality of $\mathbb{D}$, $\mathbb{U}$ and R_u are known as the DOF, uniform DOF (uDOF) and one-side uDOF [19].

This implies that the number of uncorrelated sources that a DOA estimator, i.e., SS-MUSIC, can resolve is $(\mathbb{U}-1)/2$ [5]. As such, it is desirable to design a sparse array configuration that maximizes uDOF while retaining a hole-free DCA [11].

Definition 2. *(Weight Function): The weight function $w(\ell)$ of a sparse array $\mathbb{S}$ is a number of of sensor pairs that contribute to coarray index ℓ, i.e.,*

$$w(\ell) = |\{(n_1, n_2) \in \mathbb{S}^2 | n_1 - n_2 = \ell\}|, \ \ell \in \mathbb{D}. \tag{8}$$

It is well documented [10]–[20] that the weight functions $w(1)$, $w(2)$ and $w(3)$ contribute considerably to mutual coupling effects. Thus, the smaller the values of these weight functions are, the lower the mutual coupling effect and vice versa. Hence, a perfect sparse array configuration should minimize these three weight functions.

III. Flexible ENA with Multiple Subarrays

In this section, we present the flexible ENAMS.

A. Motivation for Extension of ENAMS

The nested array consists of a union of two linear subarrays. A dense ULA made up of N_1 sensors with a unit intersensor spacing and a sparse ULA comprised of N_2 elements with intersensor spacing of $(N_1 + 1)$ [6]. In short, the sensor positions in NA can be expressed as

$$\mathbb{S}_n = \{1, 2, \ldots, N_1, (N_1 + 1), \ldots, N_2(N_1 + 1)\}. \tag{9}$$

However, the existence of a dense ULA increases the mutual coupling effect in NAs [10]. Hence, to improve the structure of NA, [20] proposed an extended NA with multiple subarrays (ENAMS).

The ENAMS consists of five subarrays where the dense-ULA of NA is split into three subarrays and the sparse ULA into two. Specifically,

$$\begin{aligned}\mathbb{S}_e =& \langle 1, N_1 - 2\rangle \cup \big(N_1 + 1\big) \cup \big(2N_2 + \langle 0, N_2 - 2\rangle (N_1 + 1)\big) \\ & \cup N_2(N_1 + 1) \cup \big(N_2(N_1 + 1) + N_1 - 2\big).\end{aligned} \tag{10}$$

Even though ENAMS extends the aperture and DOFs of NA, only two sensors are relocated from the dense ULA of NA regardless of the number of sensors N. As a result, the extended DOFs are limited compared to other state-of-the-art arrays such as MISC [18] and OS/TS-ENA [19].

In ANA [14], NA's dense ULA was grouped into right/left subarrays. Then, some sensors from the dense ULA were relocated to both sides of the sparse ULA of NA, thereby increasing the DOF and reducing the mutual coupling effect concurrently [14]. In this work, inspired by the SNA [10] and ANA [14] configurations, we extend the NA by maintaining the number of sensors in the sparse ULA of NA and splitting the dense ULA into the right/left subarrays like [14]. Then, each of the right/left subarrays is split further into dense and sparse subarrays, increasing the achievable DOF and reducing the mutual coupling effect.

B. Flexible Nested Array with Multiple Subarrays

Definition 3. *For a pair of integers $N_1 \geq 14$ and $N_2 \geq 1$, the configuration of the f−ENAMS array can be expressed as*

$$\mathbb{S} = \mathbb{S}_1 \cup \mathbb{S}_2 \cup \mathbb{S}_3 \cup \mathbb{S}_4 \cup \mathbb{S}_5, \tag{11}$$

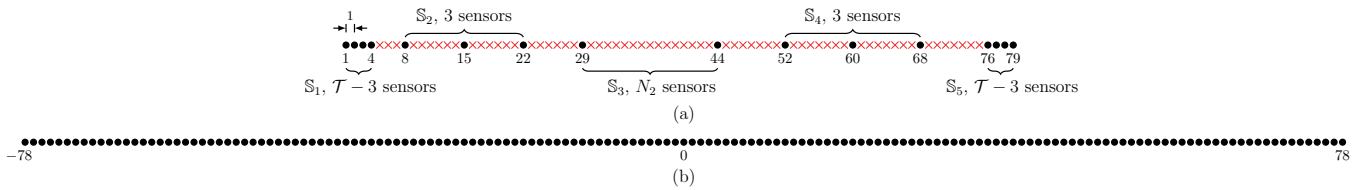

Fig. 1: A schematic representation of the flexible ENAMS array, showing all five of its component subarrays. (a) f−ENAMS array with $N_1 = 14$, $N_2 = 2$, and $N = 16$, and (b) corresponding difference co-array. •: sensors, ×: empty spaces.

$$\begin{cases} \mathbb{S}_1 = \{1 + (l_1 - 1) | 1 \le l_1 \le \mathcal{T} - 3\}, \\ \mathbb{S}_2 = \{\mathcal{T} l_2 + 1 | 1 \le l_2 \le 3\}, \\ \mathbb{S}_3 = \{(1 + l_3)(N_1 + 1) - 1 | 1 \le l_3 \le N_2\}, \\ \mathbb{S}_4 = \{N_2(N_1 + 1) + N_1 + l_4(\mathcal{T} + 1) | 1 \le l_4 \le 3\}, \\ \mathbb{S}_5 = \{N_2(N_1 + 1) + 3N_1 + 3 + l_5 | 1 \le l_5 \le \mathcal{T} - 3\}, \end{cases}$$

where $\mathcal{T} = \lfloor N_1/2 \rfloor$.

From (11), f−ENAMS consists of five subarrays where the dense ULA of the NA is split into four ULAs: $\mathbb{S}_1$, $\mathbb{S}_2$, $\mathbb{S}_4$, and $\mathbb{S}_5$. Besides, the sparse ULA of NA is retained as $\mathbb{S}_3$ with N_2 sensors. Here, $\mathbb{S}_1$ and $\mathbb{S}_5$ are made up of $\mathcal{T} - 3$ sensors with a unit spacing. Unlike ENAMS [20], $\mathbb{S}_2$ and $\mathbb{S}_4$ are not fixed to a single sensor but rather contain 3 sensors. Thus, the flexibility of these sets, coupled with a further reduction of sensors in $\mathbb{S}_1$ and $\mathbb{S}_5$, helps to improve the aperture and the achievable DOF.

Figure 1 depicts the array configuration of f−ENAMS with $N_1 = 14$ and $N_2 = 2$, and the corresponding difference co-array. Clearly, it can be observed that the number of sensors in $\mathbb{S}_2$ and $\mathbb{S}_4$ is no longer one but three sensors. Based on (11), the following property holds for f−ENAMS,

Property 1. *The DCA of f−ENAMS is hole-free, and it has a maximum uDOF of*

$$uDOF = \begin{cases} N^2/2 + 4.5N - 43 & 16 \le N \le 19 \\ N^2/2 + 4.5N - 13 & 20 \le N \le 23 \\ N^2/2 + 4.5N + 1 & N \ge 24. \end{cases} \tag{12}$$

Proof. The proof of Property 1 is given in Appendix A. □

To optimize the DOF, parameters N_1 and N_2 should be set as

$$N_1 = \begin{cases} 2\lfloor N/4 \rfloor + 6 & 16 \le N \le 19 \\ 2\lfloor N/4 \rfloor + 4 & 20 \le N \le 23 \\ 2\lfloor N/4 \rfloor + 2 & N \ge 24 \end{cases} \tag{13}$$

and $N_2 = N - N_1$. Thus, given the same number of sensors N, f−ENAMS has better DOF than [6], [16], [18]-[20].

Moreover, following (11), the weight function $w(1)$ of f−ENAMS is $N_1 - 8$ since only $N_1/2 + 1$ sensors are removed from the dense ULA of NA, and the remaining are split into two groups. Consequently, the mutual coupling due to $w(1)$ is slightly stronger in f−ENAMS than in MISC.

IV. Numerical Examples

In this section, we present numerical examples to verify the superiority of the f−ENAMS array in terms of achievable DOF and DOA estimation performance. The SS-MUSIC [21]-[22] is used for DOA estimation, and the root-mean-square error (RMSE) is adopted to quantify DOA estimation performance. In all examples, NA, improved NA, ENAMS, MISC, and TS-ENA are used for comparison purposes. For NA, ENAMS and improved NA, we select parameters $N_1 = N_2 = 11$ and $N = 22$. As for f-ENAMS, MISC and TS-ENA, we set $(N_1 = 14, N_2 = 8), (N = 22, P = 12)$ and $(N_1 = 14, N_2 = 7)$, respectively. The RMSE computed over 1000 is defined as

$$\text{RMSE} = \sqrt{\frac{1}{1000K} \sum_{q=1}^{1000} \sum_{k=1}^{K} (\tilde{\theta}_k^q - \bar{\theta}_k)^2}, \tag{14}$$

where $\tilde{\theta}_k^q$ denotes the estimate of true normalized DOA $\bar{\theta}_k$ for qth trial.

A. Achievable DOFs

In the first example, we quantitatively compare the DOF capacity of the proposed array against other kinds of extended NAs using the DOF ratio. The DOF ratio is defined as

$$\gamma(N) = N^2 / R_u(N), \tag{15}$$

where N is the number of sensors, and R_u is the one-side aperture of $\mathbb{U}$. According to (15), the smaller the $\gamma(N)$, the higher the DOF capacity, and the opposite is true [14]. Figure 2 (a) compares the DOF ratios of six kinds of extended NAs. NA has the highest values of $\gamma(N)$, while the f−ENAMS has the lowest possible values, except when $N < 19$. This is due to the restriction on the value of N_1 as shown in (13) to guarantee a hole-free coarray. Hence, the achievable DOF of f−ENAMS when $N < 19$ is limited. Meanwhile, the $\gamma(N)$ values of TS-ENA, MISC, ENAMS, NA, and improved NA follow those of f−ENAMS in that order.

B. DOA Estimation Performance

In the second example, we evaluate the DOA estimation performance of the proposed f−ENAMS against other sparse arrays. We compute the RMSE versus the input SNR when $K = 50$ sources are located at $\bar{\theta}_k = -0.3 + 0.6(k-1)/49$ for $1 \le k \le 50$. The number of snapshots is fixed at 1000 while the input SNR varies from −30 to 10 dB. Figure 2 (b) compares the RMSE performance of six kinds of NAs.

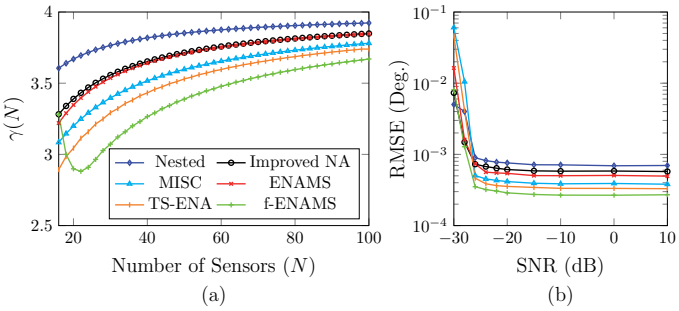

(a) (b)

Fig. 2: (a) The DOF ratio $\gamma(N)$ for $18 \leq N \leq 100$. (b) RMSE of DOA estimates versus the input SNR.

TABLE I: Optimal DOF of Various Sparse Arrays

Non-uniform Array	Optimal N_1	Maximum DOF
Nested [6]	$N/2$	$N^2/2+N-1$
Improved Nested [16]	$N/2$	$N^2/2+2N-3$
ENAMS [20]	$N/2$	$N^2/2+2N-1$
MISC [18]	$2\lfloor N/4 \rfloor+1$	$N^2/2+3N-9$
TS-ENA [19]	$2\lfloor (N+3)/4 \rfloor$	$N^2/2+3.5N-1$
f−ENAMS	$2\lfloor N/4 \rfloor+2$	$N^2/2+4.5N+1$

As shown in Fig. 2 (b), NA performs poorly, followed by improved NA due to limited DOF. However, f−ENAMS outperforms the ENAMS, MISC, and TS-ENA arrays. Thus, the improved DOF of f−ENAMS enhances the DOA estimation performance.

V. Conclusion

This paper presented a flexible ENAMS array design with enhanced DOF and hole-free co-array. Besides, the array geometry has closed-form expressions for sensor positions. Simulation examples demonstrated that the proposed f−ENAMS offers high-resolution DOA estimation performance compared to other state-of-the-art extended NAs.

Appendix A
Proof of Property 1

The proposition that the DCA of f−ENAMS has a $\mathbb{U}$ in $\langle -L_u+7N_1/2-1, L_u+7N_1/2-1\rangle$ where $L_u = N_2(N_1+1)$ is equivalent to the argument that for $n \in \mathbb{U}$, there exists at least one pair of sensors that leads to it, and since DCA is symmetric about the origin, then it suffices to show that $0 \leq n \leq L_u+7N_1/2-1$. As such, we consider the following cases:

a) Case 1: The lags in the range $\langle 0, 3N_1/2\rangle$ can be realized by taking the union of $\xi(\mathbb{S}_2,\mathbb{S}_1)$ and $\xi(\mathbb{S}_5,\mathbb{S}_4)$. Namely,

$$\xi(\mathbb{S}_2,\mathbb{S}_1) \approx \langle 0,\mathcal{T}\rangle \cup \big(N_1 - \langle 1,3\rangle\big) \cup (3N_1/2 - \langle 1,3\rangle).$$

$$\xi(\mathbb{S}_5,\mathbb{S}_4) \approx \langle 0,\mathcal{T}-4\rangle \cup \langle \mathcal{T}, N_1-2\rangle \cup \big(N_1 - \langle 1, N_1/2-3\rangle\big) \cup \big(2(N_1+1) + \langle 1,\mathcal{T}-3\rangle\big).$$

Thus, collectively $\xi(\mathbb{S}_2,\mathbb{S}_1)$ and $\xi(\mathbb{S}_5,\mathbb{S}_4)$ covers the lags between $\mathbb{S}_1$ and $\mathbb{S}_2$.

b) Case 2: The lags in the range $\langle 3N_1/2, L_u+N_1-1\rangle$ can be realized by taking the union of $\xi(\mathbb{S}_3,\mathbb{S}_1)$, $\xi(\mathbb{S}_3,\mathbb{S}_2)$, $\xi(\mathbb{S}_3,\mathbb{S}_4)$, $\xi(\mathbb{S}_3,\mathbb{S}_5)$ and $\xi(\mathbb{S}_4,\mathbb{S}_2)$, such that

$$\xi(\mathbb{S}_3,\mathbb{S}_1) \approx \langle 0,\mathcal{T}-4\rangle \cup \big(2(N_1+1) - \langle 2,\mathcal{T}-2\rangle\big) \cup \big(L_u+N_1 - \langle 1,\mathcal{T}-4\rangle\big).$$

$$\xi(\mathbb{S}_3,\mathbb{S}_2) \approx \mathcal{T}\langle 0,1\rangle \cup \big(N_1+\langle 0,1\rangle\big) \cup \big(N_1/2+\langle 0,1\rangle\big) \cup \big(L_u+3N_1/2-1\rangle\big).$$

$$\xi(\mathbb{S}_3,\mathbb{S}_4) \approx \big(0,\mathcal{T}+1\big) \cup \big(N_1+\langle 1,2\rangle\big) \cup \big(N_1/2+\langle 2,3\rangle\big) \cup \big(2(N_1+1)+(\mathcal{T}+1)\langle 0,1\rangle+1\big).$$

$$\xi(\mathbb{S}_3,\mathbb{S}_5) \approx \langle 0,\mathcal{T}-4\rangle \cup \big(N_1+1\big) \cup \big(2(N_1+1)+3\langle 1,2\rangle\big) \cup \big(N_u+N_1+\langle 1,\mathcal{T}-3\rangle+3\big).$$

$$\xi(\mathbb{S}_4,\mathbb{S}_2) \approx \mathcal{T}\langle 1,2\rangle \cup (\mathcal{T}+1)\langle 1,2\rangle \cup \big(2(N_1+1)+\mathcal{T}+\langle 1,2\rangle\big) \cup \big(L_u+N_1+\langle 1,\mathcal{T}-4\rangle\big) \cup \big(L_u+3N_1/2+\langle 1,2\rangle\big) \cup \big(L_u+2N_1+2\big).$$

Thus, the union of the five sets covers the lags between the end of $\mathbb{S}_2$ to $\mathbb{S}_3$.

c) Case 3: Considering the lags in $\langle L_u+N_1, L_u+5N_1/2+3\rangle$, these lags span the section beginning from end of $\mathbb{S}_3$ and the end of set $\mathbb{S}_4$. This section can be filled by the union of sets $\xi(\mathbb{S}_4,\mathbb{S}_1)$, $\xi(\mathbb{S}_5,\mathbb{S}_2)$ and some fragments from *Case 2* where

$$\xi(\mathbb{S}_4,\mathbb{S}_1) \approx \langle 0,\mathcal{T}-4\rangle \cup \big(L_u+3N_1/2-\langle 1,\mathcal{T}-3\rangle\big) \cup (\mathcal{T}+1)\langle 1,2\rangle \cup \big(L_u+2N_1-\langle 1,\mathcal{T}-3\rangle-1\big) \cup \big(L_u+5N_1/2+3-\langle 1,\mathcal{T}-3\rangle\big).$$

$$\xi(\mathbb{S}_5,\mathbb{S}_2) \approx \langle 0,\mathcal{T}-4\rangle \cup \langle N_u+2N_1-4, L_u+2N_1-1\rangle \cup \langle L_u+5N_1/2-4, L_u+5N_1/2-1\rangle \cup \langle L_u+5N_1/2+3, L_u+3N_1-1\rangle.$$

Combining these two sets with segments from $\xi(\mathbb{S}_3,\mathbb{S}_1)$, $\xi(\mathbb{S}_3,\mathbb{S}_2)$, $\xi(\mathbb{S}_4,\mathbb{S}_2)$ and $\xi(\mathbb{S}_3,\mathbb{S}_5)$ yields the lags in the range $\langle L_u+N_1, L_u+5N_1/2+3\rangle$.

d) Case 4: Finally, the lags in $\langle L_u+3N_1, N_u+7N_1/2-1\rangle$ can be generated from the sets $\xi(\mathbb{S}_5,\mathbb{S}_1)$ and $\xi(\mathbb{S}_5,\mathbb{S}_2)$, such that

$$\xi(\mathbb{S}_5,\mathbb{S}_1) \approx \langle 0,\mathcal{T}-4\rangle \cup \langle L_u+3N_1, L_u+7N_1/2-1\rangle.$$

It can be observed that all the lags in $\langle L_u+3N_1, L_u+7N_1/2-1\rangle$ are covered by the two sets.

In general, the union of *Cases (1)-(4)* cover the consecutive integers in $\langle 0, L_u+7N_1/2-1\rangle$, i.e., the DCA of f−ENAMS is hole-free. Accordingly, the R_u of f−ENAMS is $\langle 0, L_u+7N_1/2-1\rangle$, assuming that $\lfloor N_1/2 \rfloor$ and $\lfloor N/4 \rfloor$ are $N_1/2$ and $N/4$, respectively. The $\mathbb{U}$ of f−ENAMS can be expressed as $2R_u+1 \approx 2N_2(N_1+1)+7N_1-1$. As such, maximizing the uDOF under the constraint of $N = N_1+N_2$ yields $N^2/2+4.5N-43$, $N^2/2+4.5N-13$ and $N^2/2+4.5N+1$ given that $2\lfloor N/4 \rfloor+6$, $2\lfloor N/4 \rfloor+4$ and $2\lfloor N/4 \rfloor+2$ in that order and $N_2 = N-N_1$. Therefore, Property 1 is proved.

REFERENCES

[1] T. E. Tuncer and B. Friedlander, "Classical and modern direction of arrival estimation," *Academic Press*, 2009.

[2] P. Chevalier, L. Albera, A. Ferrool, P. Common, "On the virtual array concept for higher-order array processing," *IEEE Trans. Signal Processing*, vol. 53, no.4, pp. 1254-1271, Sep. 2005.

[3] A. Moffet, "Minimum-redundancy linear arrays," *IEEE Trans. Antennas Propagation*, vol. 16, no. 2, pp. 172-175, Mar. 1968.

[4] E. Vertatschitsch and S. Haykin, "Non-redundancy arrays," *Proc. in IEEE*, vol. 74, no.1, pp. 217-217, Jan. 1986.

[5] P. P. Vaidyanathan and P. Pal, "Sparse sensing with co-prime samplers and arrays," *IEEE Trans. Signal Processing*, vol. 59, no. 2, pp. 573-586, Feb. 2011.

[6] P. Pal and P. P. Vaidyanathan, "Nested arrays: A novel approach to array processing with enhanced degrees of freedom," *IEEE Trans. Signal Processing*, vol. 58, no. 8, pp. 4167-4181, Aug. 2010.

[7] S. Wandale and K. Ichige, "Design of sparse arrays via deep learning for enhanced DOA estimation." *EURASIP J. Adv. Signal Process*, no. 2021(1):17, Apr. 2021.

[8] S. Wandale and K. Ichige, "Simulated Annealing Assisted Sparse Array Selection Utilizing Deep Learning," *IEEE Access*, vol. 9, pp. 156907-156914, 2021.

[9] S. Nakamura, S. Iwazaki and K. Ichige, "Optimization and Hole Interpolation of 2-D Sparse Arrays for Accurate Direction-of-Arrival Estimation," *IEICE Trans. Communications*, vol. E104-B, no. 4, pp. 401-409, Apr. 2021.

[10] C. Liu and P. P. Vaidyanathan, "Super nested arrays: Linear sparse arrays with reduced mutual coupling-Part I: Fundamentals," *IEEE Trans. Signal Processing*, vol. 64, no. 15, pp.3997-4014, Aug. 2016.

[11] J. Shi, G. Hu, X. Zhang, and H. Zhou, "Generalized Nested Array: Optimization for Degrees of Freedom and Mutual Coupling," *IEEE Communications Letters*, vol. 22, no. 6, pp. 1208-1211, Jun. 2018.

[12] S. Qin, Y. D. Zhang, and M. G. Amin, "Generalized co–prime Array Configurations for Direction-of-Arrival Estimation," *IEEE Transactions on Signal Processing*, vol. 63, no. 6, pp. 1377-1390, Mar. 2015.

[13] A. Raza, W. Liu, and Q. Shen, "Thinned co-prime arrays for DOA estimation," *Proc. of 2017 25th European Signal Processing Conference (EUSIPCO)*, pp. 395-399, 2017.

[14] J. Liu, Y. Zhang, Y. Lu, S. Ren, and S. Cao, "Augmented nested arrays with enhanced DOF and reduced mutual coupling," *IEEE Transactions on Signal Processing*, vol. 65, no. 21, pp. 5549-5563, Nov. 2017.

[15] P. Zhao, G. Hu, Z. Qu, and L. Wang, "Enhanced Nested Array Configuration With Hole-Free Co-Array and Increasing Degrees of Freedom for DOA Estimation," *IEEE Communications Letters*, vol. 23, no. 12, pp. 2224-2228, Dec. 2019.

[16] Y. Minglei, S. Lei, Y. Xin, and C.Baixiao, "Improved nested array with hole-free DCA and more degrees of freedom," *Electronics Letters*, vol. 52, no. 25, p. 2068-2070, Dec. 2016.

[17] Y. Iizuka and K. Ichige, "Extension of Nested Array for Large Aperture and High Degree of Freedom," *IEICE Communication Express*, vol. 6, no. 6, pp. 381-386, Jun. 2017.

[18] Z. Zheng, W. Wang, Y. Kong and Y. D. Zhang, "MISC Array: A New Sparse Array Design Achieving Increased Degrees of Freedom and Reduced Mutual Coupling Effect," *IEEE Transactions on Signal Processing*, vol. 67, no. 7, pp. 1728-1741, Apr. 2019.

[19] S. Ren, W. Dong, X. Li, W. Wang, and X. Li, "Extended Nested Arrays for Consecutive Virtual Aperture Enhancement," *IEEE Signal Processing Letters*, vol. 27, pp. 575-579, 2020.

[20] S. Wandale and K. Ichige, "A Nested Array Geometry with Enhanced Degrees of Freedom and Hole-Free Difference Coarray," *Proc. of 29th European Signal Processing Conference (EUSIPCO)*, pp. 1905-1909, Aug. 2021.

[21] C. Liu and P. P. Vaidyanathan, "Remarks on the Spatial Smoothing Step in Coarray MUSIC," *IEEE Signal Processing Letters*, vol. 22, no. 9, pp. 1438-1442, Sept. 2015.

[22] Z. Tan, Y. C. Eldar, and A. Nehorai, "Direction of arrival estimation using co-prime arrays: A super resolution viewpoint," *IEEE Transactions on Signal Processing*, vol. 62, no. 21, pp. 5565–5576, Nov. 2014.